Available online at www.sciencedirect.com
SCIENCE DIRECT®
Carbohydrate Research 339 (2004) 2391–2405
Carbohydrate RESEARCH

The complexation of metal cations by D-galacturonic acid: a spectroscopic study

Andriy Synytsya,[a,*] Marie Urbanová,[b] Vladimír Setnička,[c] Marcela Tkadlecová,[c] Jaroslav Havlíček,[c] Ivan Raich,[d] Pavel Matějka,[c] Alla Synytsya,[c] Jana Čopíková[a] and Karel Volka[c]

[a]*Department of Carbohydrate Chemistry and Technology, Institute of Chemical Technology, Technická 3/5, 166 28 Prague 6, Czech Republic*
[b]*Department of Physics and Measurements, Institute of Chemical Technology, Technická 3/5, 166 28 Prague 6, Czech Republic*
[c]*Department of Analytical Chemistry, Institute of Chemical Technology, Technická 3/5, 166 28 Prague 6, Czech Republic*
[d]*Department of Chemistry of Natural Compounds, Institute of Chemical Technology, Technická 3/5, 166 28 Prague 6, Czech Republic*

Received 30 August 2002; received in revised form 16 June 2004; accepted 8 July 2004
Available online 9 September 2004

Abstract—Solid complexes of D-galacturonic acid (GalA) with cobalt(II), copper(II), nickel(II) and oxovanadium(IV) (**1**–**4**) were prepared and characterised. The metal-to-ligand molar ratio was 1:2 for complexes **1**–**3** and 1:1 for complex **4**. The α- and β-anomers of GalA were detected in all the complexes in solid state and in solutions. An addition of small amounts of the paramagnetic complexes to the D_2O solution of pure ligand led to NMR line broadening of some ^1H and ^{13}C nuclei. This broadening was sensitive to the anomeric state of GalA in the case of complexes **1** and **4**. NMR and vibrational spectroscopic data indicate the formation of carboxylate complexes of all the cations, while noncarboxylic oxygens are also involved into the metal bonding in some cases. VCD spectra of complexes **1**–**4** in D_2O and Me_2SO-d_6 solutions confirm that GalA carboxylic group may participate in the formation of optically active species around the metal cation. Possible ways of GalA coordination by metal cations of this study were proposed and discussed.

Keywords: Galacturonic acid; Metal complexes; Electronic spectroscopy; ^1H and ^{13}C NMR spectroscopy; FT-IR and Raman spectroscopy; Vibrational circular dichroism

1. Introduction

Pectins are common plant polysaccharides that have various applications in the food industry and pharmacy.[1] The structural basis of these polysaccharides is linear partially methyl esterified galacturonan, a polymer of 1,4-α linked D-galacturonic acid (GalA) units. Free carboxylic groups of pectins are able to strongly bind polyvalent metal cations.[2,3] This property is important for Ca^{2+}-dependent gelation of low-methoxy pectins[4–6] as well as for removing toxic heavy metals from the human body by indigestible pectic fibres.[7]

GalA and its oligomers has been used as a simple model of pectin in the study of biologically important interactions with polyvalent metal cations.[8–33] On the other hand, GalA itself represents an example of a functionalised sugar demonstrating good complexation properties.[9,10] The pH-dependent interactions of GalA with copper(II),[11–13] cobalt(II),[14] nickel(II),[14] oxovanadium(IV)[13,15] and lanthanide[16–20] cations in aqueous solution have been studied by potentiometry and spectroscopic methods. Several ways of GalA binding to metal cations have been suggested: only through the carboxylate[19,21] as well as with the additional coordination on the O-5 atom[19,20,22–24] or on one of the hydroxyls.[25,26] The reduction of iron(III),[27–29] vanadium(V)[30,31] and chromium(IV)[32,33] by GalA and/

* Corresponding author. Tel.: +42-02-24353114; e-mail: sinicaa@vscht.cz

0008-6215/$ - see front matter © 2004 Elsevier Ltd. All rights reserved.
doi:10.1016/j.carres.2004.07.008

or metal/GalA complexes has also been investigated. However, only several publications have been devoted to preparation and analysis of solid GalA complexes with metal cations.[18,34,35]

In the present work a facile approach for the preparation of metal/GalA complexes is described by the reaction of the ligand with an excess of freshly prepared metal hydroxide. The solid complexes of GalA with cobalt(II), copper(II), nickel(II) and oxovanadium(IV) were prepared and characterised by spectroscopic methods. Chiroptical properties of these complexes were analysed by vibrational circular dichroism (VCD) spectroscopy.

2. Results

2.1. Composition of the metal–galacturonate complexes

The metal complexes of GalA were prepared as described in the experimental section. The complexation proceeded in aqueous solution according to the following equations:

$$M^{2+} + OH^- \rightarrow M(OH)_2 \downarrow$$
$$n\text{GalA} + M(OH)_2 \rightarrow M \cdot (\text{GalA})_n$$

where M stands for Co^{2+}, Cu^{2+}, Ni^{2+} and VO^{2+} cations. According to elemental analysis (Table 1), the metal-to-ligand molar ratio was 1:1 for the oxovanadium(IV) complex ($n = 1$) and 1:2 for the other complexes ($n = 2$). The analysis of organic elements (C, H), metals and water reveals the following stoichiometry of the solid complexes: Co(D-GalA)$_2$·5H$_2$O (**1**), Cu(D-GalA)$_2$·4H$_2$O (**2**), Ni(D-GalA)$_2$·4H$_2$O (**3**), VO(D-GalA)·2H$_2$O (**4**).

2.2. Electronic spectra

The electronic reflectance spectra of the solid complexes are shown in Figure 1. The electronic spectra band maxima and their assignment in solution and solid state are presented in Table 2. The band positions of complexes **1**–**3** are typical of a pseudo-octahedral configuration,[36] whereas oxovanadium(IV) cation of complex **4** showed electronic bands typical of distorted tetragonal pyramid.[36–38] Surprisingly, the electronic absorption spectra of complex **2** in Me_2SO and complex **3** in H_2O showed significant changes in absorbance during several hours after dissolving (Fig. 2). The absorbance at 740 nm of complex **2** in Me_2SO significantly decreased during first 1.5 h, while a new absorbance shoulder at 410 nm appeared and increased until 4 h after dissolving (Fig. 2a). A freshly prepared aqueous solution of complex **3** showed an intense absorption at 354 nm that disappeared during the first 1.5 h (Fig. 2b), while the visible bands of nickel(II) at 657 and 710 nm (shoulder) were not altered (not shown). These spectroscopic changes indicate that, in both these cases, the complexes are non-stable in the appropriate solvents (Me_2SO for **2**, H_2O for **3**). Therefore, the structural implications obtained from the corresponding solution measurements cannot be adequately extrapolated to the solid state of these complexes. In all the other cases the absorption values of characteristic metal peaks did not change significantly during several hours after dissolving, so the complexes were stable in the solutions.

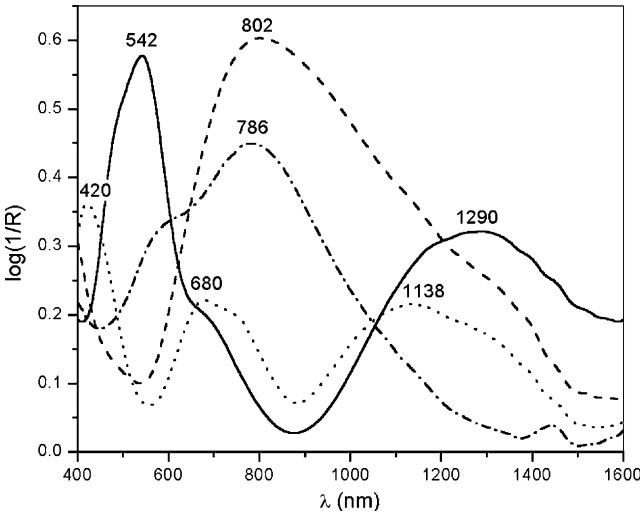

Figure 1. vis/NIR reflectance spectra of metal/GalA complexes **1** (—), **2** (----), **3** (····) and **4** (-·-·-).

2.3. NMR spectroscopic study

The ^1H and ^{13}C NMR spectra of GalA equilibrated in D_2O at pH 5.5 consist of a number of discrete resonance

Table 1. Content (in % m/m) of organic elements (C, H), metal cations[a] and water in metal/GalA complexes **1**–**4**

Complex	Molecular formula	C		H		Metal		H_2O	
		Calcd	Exp.	Calcd	Exp.	Calcd	Exp.	Calcd	Exp.
1	$C_{12}H_{28}O_{19}Co$	26.92	27.09	5.23	5.31	11.02	11.15	16.82	17.31
2	$C_{12}H_{26}O_{18}Cu$	27.61	27.32	4.99	4.92	12.18	12.42	13.81	14.54
3	$C_{12}H_{26}O_{18}Ni$	27.87	27.36	5.03	4.80	11.36	11.74	13.93	13.79
4	$C_6H_{13}O_{10}V$	24.33	24.49	4.39	4.58	17.21	17.10	12.16	12.36

[a] Co^{2+} for **1**, Cu^{2+} for **2**, Ni^{2+} for **3**, VO^{2+} for **4**.

Table 2. Electronic spectra of the metal complexes of GalA

Complex	Wavelength (nm)[b]			Assignment	Configuration
	Aqueous solution	Me_2SO solution	Diffuse reflectance		
1	508	539, 688sh	542, 692sh	$^4T_{1g}(F) \rightarrow {}^4T_{1g}(P)$	O_h with C_{4v} distortion
			1290	$^4T_{1g}(F) \rightarrow {}^4T_{2g}(P)$	
2		410sh[a]		CT	Distorted O_h
	785	740[a]	802	$^2E_g \rightarrow {}^2T_{2g}$	
3	352[a]	403sh	420	$^3A_{2g} \rightarrow {}^3T_{1g}(P)$	Distorted O_h
	657	684	680	$^3A_{2g} \rightarrow {}^1E_g$	
	710sh	748	764sh	$^3A_{2g} \rightarrow {}^3T_{1g}(F)$	
			1138	$^3A_{2g} \rightarrow {}^3T_{2g}$	
4	354sh	409sh		$^2B_2 \rightarrow {}^2A_1$	Distorted C_{4v}
	543sh	533sh, 632	566sh	$^2B_2 \rightarrow {}^2B_1$	
	735	775sh	786	$^2B_2 \rightarrow {}^2E$	

[a] Intensity of these bands changes significantly after dissolving.
[b] sh, shoulder.

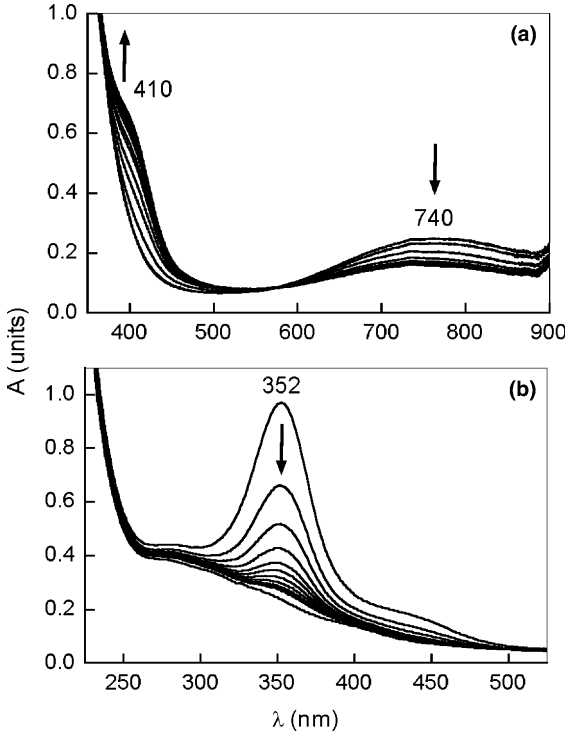

Figure 2. UV/VIS absorption spectra of copper(II)/GalA complex **2** in Me_2SO solution (a) and of nickel(II)/GalA complex **3** in aqueous solution (b) recorded each 20 min during 5 h after dissolving.

signals (10 protons and 12 carbons) owing to the presence of two anomers, α and β (Fig. 3a and b). The assignments for these resonances were made according to the literature.[39] Corresponding NMR spectra of the metal/GalA complexes exhibited broad featureless envelopes with loss of fine structure due to the presence of large amount of paramagnetic cations. Therefore, the detailed assignment of these spectra was not possible. However, the selective broadening of NMR peaks arising from a decrease in the transverse relaxation time due to complexation of paramagnetic ion can give qualitative information about possible binding sites.[12] Thus, paramagnetic metal complexes of GalA were added in a small quantity (1:1000 and 1:100 mol/mol) to the D_2O solution of free ligand and the effect of the paramagnetic cations on the broadening of the ligand nuclei was analysed: an addition of complex **1** to free ligand at the molar ratio of 1:1000 led to significant broadening of specific NMR signal, while no detectable changes were observed for the other complexes at the same conditions. An higher order amount of these complexes (1:100 mol/mol) was added to obtain marked broadening. (Fig. 3, Table 3). In all cases, significant broadening of C-6 and C-5 signals of both α- and β-anomers was detected after an addition of the complexes. This confirms that GalA carboxylates participate in the binding of all the cations. Specific broadening of other nuclei of the ligand was also observed in some cases confirming that noncarboxylate sites can be involved into the coordination by metal.

The paramagnetic complexes differ significantly in their effects on the protons and the other carbons of GalA. Moreover, in some cases these effects depended on the anomeric state of the ligand. It can be seen, for example that the protons H-1, H-2, H-4 and H-5 and carbons C-1, C-2 and C-4 did broaden significantly only for α-GalA when complex **1** was added (Fig. 3a and b). Addition of complexes **2** and **3** lead to nonspecific broadening of all protons and carbons with exception of C-5 and C-6. In the case of complex **4** the C-1 carbon of α-GalA and the H-5 and C-4–C-6 nuclei of both anomers showed specific broadening of NMR signals. However, the decrease of the C-4 carbon signal of α- and β-GalA anomers was less pronounced for complexes **1** and **4**, respectively (Table 3).

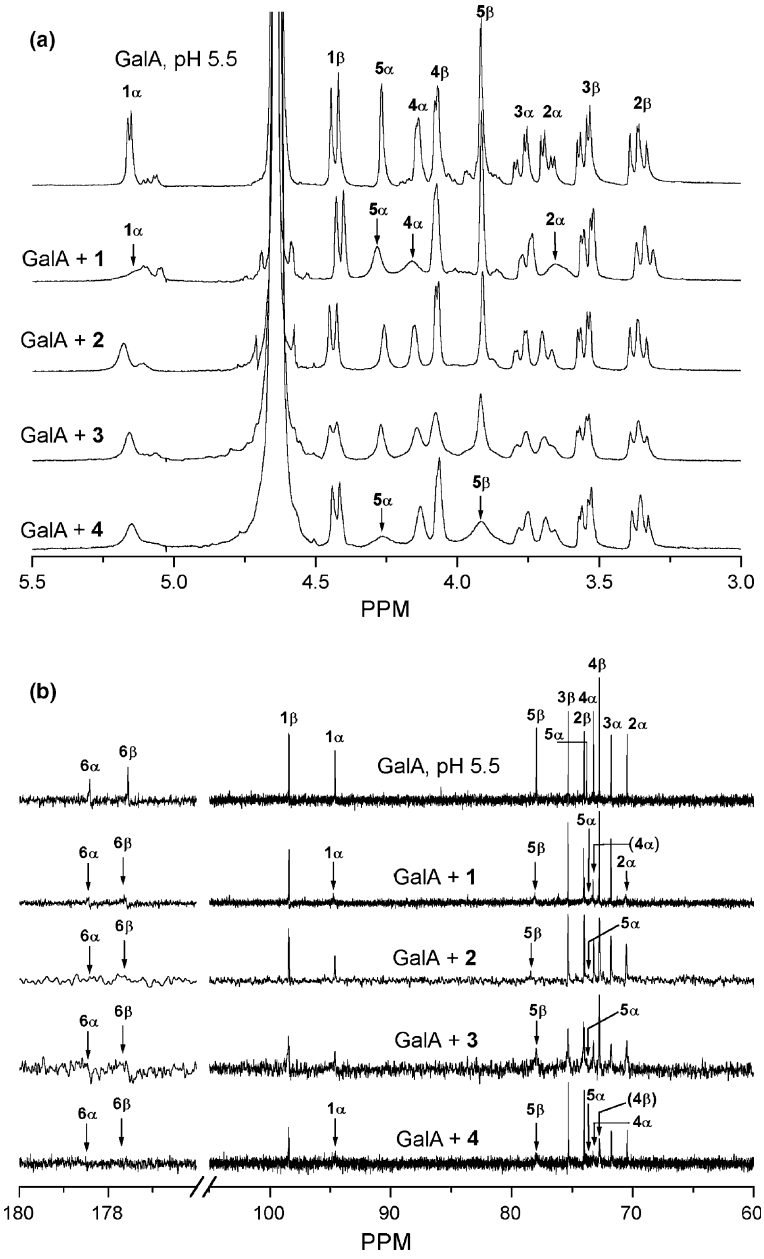

Figure 3. ^{1}H NMR (a) and ^{13}C NMR (b) spectra of GalA·H_2O alone and with an addition of metal/GalA complexes **1**–**4** (1:1000 mol/mol for complex **1**, 1:100 mol/mol for the other complexes) in D_2O, pH 5.5.

2.4. Vibration spectroscopic study in solid state

Diffuse reflection FT-IR, FT-Raman and Vis–Raman spectra of the metal/GalA complexes and of free ligand in solid state are shown in Figures 4 and 5. The band assignment is presented in Table 4. In the spectral region of 3700–2500 cm^{-1} the IR spectrum of GalA·H_2O shows four groups of bands: 3700–3000 cm^{-1} (OH stretching vibrations of water and hydroxyls), 2980–2910 cm^{-1} (CH stretching vibrations), 2860–2710 cm^{-1} (overtones) and 2610–2490 cm^{-1} (OH stretching of COOH dimers). The complexes show a broad IR band at 3700–3000 cm^{-1} with a shoulder at lower frequency (Fig. 4a). Occurrence of the shoulder is probably caused by the presence of additional water molecules in the complexes and (or) the changes in H-bonding network of the free ligand upon complexation.[40–42] The last group of bands (2610–2490 cm^{-1}) is absent in the complexes confirming ionisation of GalA carboxyls.[40] Vibrational spectra of GalA·H_2O shows three C–H stretching bands, which are weak in IR and strong in Raman (Fig. 4). The complexes show only one broadened band shifted to a lower frequency in comparing with the main maximum at ~2955 cm^{-1} of GalA. Both the broadening and the shift observed could be related to the presence of several ligand species, including β-anomers, bound to metal cations.[43,44]

Table 3. Broadening of the ^{1}H and ^{13}C NMR signals[a] of GalA after addition (1:1000 mol/mol for **1**, 1:100 mol/mol for **2**–**4**) of the paramagnetic complexes **1**–**4**

	Metal	H-1α	H-2α	H-3α	H-4α	H-5α		H-1β	H-2β	H-3β	H-4β	H-5β	
1	Co^{2+}	++	++		++	++							
2	Cu^{2+}												
3	Ni^{2+}												
4	VO^{2+}					++						++	
		C-1α	C-2α	C-3α	C-4α	C-5α	C-6α	C-1β	C-2β	C-3β	C-4β	C-5β	C-6β
1	Co^{2+}	++	++		+	++	++					++	++
2	Cu^{2+}					++	++					++	++
3	Ni^{2+}					++	++					++	++
4	VO^{2+}	++			++	++	++				+	++	++

[a] ++, strong specific broadening; +, less pronounced specific broadening.

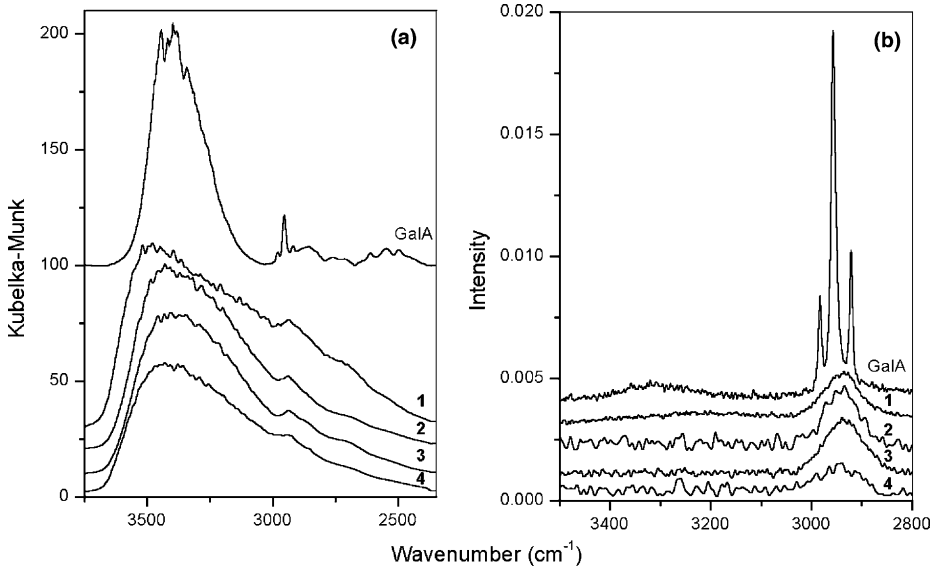

Figure 4. Diffuse reflectance FT-IR (a) and FT-Raman (b) spectra of GalA·H_2O and its metal complexes **1**–**4** in the region of 4000–2000 cm^{-1}.

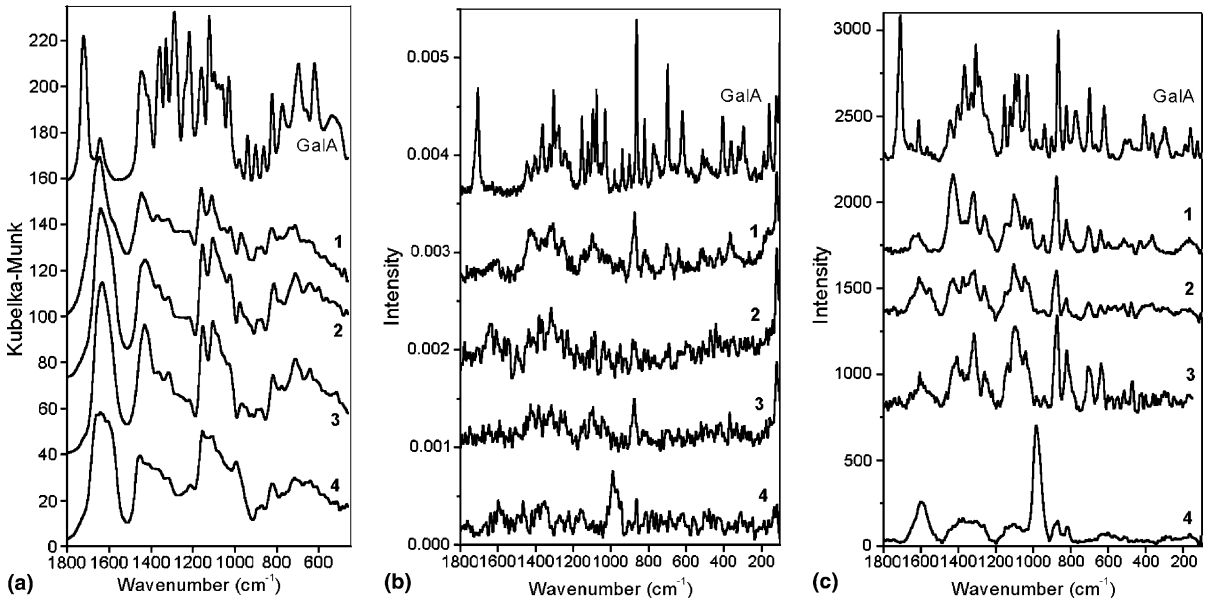

Figure 5. Diffuse reflectance FT-IR (a), FT-Raman (b) and Vis–Raman (c) spectra of GalA·H_2O and its metal complexes **1**–**4** in the region below 1800 cm^{-1}.

Table 4. Vibration band positions (in cm^{-1}) and their assignments for the metal complexes of GalA **1**–**4** in comparison with those of free ligand[40–53]

D-GalA H_2O			**1**			**2**			**3**			**4**			Assignments
FT-IR	FT-R	vis–R	FT-IR	FT-R	vis–R	FT-IR	FT-R	vis–R	FT-IR	FT-R	vis–R	FT-IR	FT-R	vis–R	
3443			3469			3415						3418			ν(OH) ring, $\nu(H_2O)$
3396									3395						ν(OH) ring, $\nu(H_2O)$
3342															ν(OH) ring, $\nu(H_2O)$
2980	2982														$\nu(C_1–H)$ α-anomer
2954	2956		2934	2935		2939	2934		2937	2939	2936	2945	2948	2938	$\nu(C_{2,3,4}–H)$
2919	2921														$\nu(C_5–H)$
2856															Overtones
2763															Overtones
2713															Overtones
2609															ν(OH) acid, overtones
2547															ν(OH) acid, overtones
2497															ν(OH) acid, overtones
1722	1707	1709													ν(C=O) acid
1642			1646			1641			1642			1642			$\delta(H_2O)$
			1606	1606	1614		1610	1612			1606	1608	1599	1600	$\nu_{as}(COO^-)$
			1468									1467	1467		δ(COH) + δ(CCH)
1445	1446	1444	1445			1452			1452			1450			δ(COH) + δ(CCH)
1418			1427	1425	1429	1429	1437	1429	1433	1426	1430	1429		1429	δ(CCH) + δ(COH)
			1409			1413	1414		1412		1408	1410			$\nu_s(COO^-)$
						1393								1397	$\nu_s(COO^-)$
	1405	1402													δ(COH) acid
1359	1362	1368	1370	1370		1365	1382	1378	1365	1384	1380	1382	1353	1376	δ(CCH) + δ(COH)
1329	1328	1330	1318	1326	1320	1317	1318	1315	1316	1316	1317	1311		1309	δ(COH) + δ(OCH)
	1305	1306													δ(COH) + δ(OCH)
1289	1276	1289	1259	1259	1260	1246	1262	1263	1276	1266	1260		1271	1264	δ(COH) + δ(OCH)
1243	1244	1254	1239			1244	1232		1244	1244		1242			δ(COH) + δ(CCH)
1218			1222			1220			1213		1190	1213	1224		ν(CC) + δ(COH)
1160	1154	1155	1160	1143	1150	1155	1183	1150	1155	1140	1138	1155	1161	1146	ν_{as}(C–O–C)
1123	1122	1123	1111				1127							1125	ν(CO) + ν(COC)
1099	1097	1097		1098	1104	1106		1106	1108	1095	1097	1108	1094	1106	ν(CO) + ν(CC)
1077	1077	1079	1086			1080	1086		1075			1082		1072	ν(CO) + ν(CC)
1057			1050	1048	1048	1053	1038	1046	1051	1048	1041	1042		1035	ν(CO) + ν(CC)
1030	1031	1033	1022		1014	1025	1011	1024	1024			1024			ν(CO) + ν(CC)
												995	990	985	ν(V=O)
980	981	985	971			977		989	968		983	965			ν(CO) + δ(CCO)
940	939	940	946	954	948	952	951	946	948	944	941				δ(CO) + ν(CCH)
			923			926	930		920						$\delta(COO^-)$
902	903	902													δ(CC) + ν(CO)
			894			890	885		894			889			$\delta(C_1–H)$ β-anomer
863	864	866	874	874	876	875	871	875	873	876	873	873	864	870	τ(CO) α-anomer
823	821	823	824	819	823	815		823	821		821	821	812	819	$\delta(C_1–H)$ α-anomer
774	773	773	787			782		773	776			774	760		ν_s(C–O–C)
698	698	700	713	704	708	714	692	707	715	697	708	715	689	702	$\tau(C_1O_1)$ α-anomer, $\rho(H_2O)$
	661	663	673									663			τ(CCO) + δ(CCO)

620											635		τ(CCO), ω(H_2O)
	620	622	647	639	641	643		641	640		602		τ(CCO) + δ(CCO)
			604	589	600	601	602	602	574	593	610		τ(CO) + δ(CCO)
	575	577	573			565		560	555		533	563	δ(CCO) + τ(CO)
537	512	512	527	511	518		534	517	517	521	515		δ(CCO) + τ(CO)
	489	487	504				511		491	493			ν(V–O)
			478	474	474	474	472	478		470	472	478	τ(C_1O_1) β-anomer
	441	451		427	431		443	419		416	421	433	δ(CCO) + δ(CCH)
	406	407					398				402	375	δ(CCO), δ(CCH)
	360	363		366	366		349	365		369	360		δ(CCO)
	323						312	308		331		309	δ(CCO)
	295	298						283		291	300		δ(CCO)
	234	238		265			246				251	246	τ(CC) + τ(CO)
	188	190						192			212		τ(CC) + τ(CO)
	158	162		163	169			166			178	185	τ(CC) + τ(CO)
		123		119			118			119			τ(CC) + τ(CO)

A strong vibration band at 1722 cm^{-1} (FT-IR) or ~1708 cm^{-1} (Raman) of the free ligand, assigned to the C=O stretching vibration of COOH, was shifted to a lower frequency and separated into two components: ~1606 cm^{-1} (antisymmetric stretching of COO^-) and ~1410 cm^{-1} (symmetric stretching of COO^-) (Fig. 5). These spectral changes confirm that the carboxylic groups are ionised in the complexes and therefore can bind metal cations.[18,45–51] The former IR band of COO^- is overlapped by the bending vibration band of water $\delta(H_2O)$ at ~1640 cm^{-1}.

The IR/Raman bands at 1460–1200 cm^{-1} (Fig. 5) were assigned to CCO, COH and CCH bending vibrations. These bands showed considerable changes in intensity and position upon complexation. Free acid has two bands at ~1445 and ~1405 cm^{-1} (shoulder in IR). In the complexes, new bands arise at ~1430 and 1410–1390 cm^{-1}. The complexes **1** and **4** also have a band or shoulder at 1468 cm^{-1} that could appear due to some conformational changes in the pyranoid ring upon complexation. The bands at 1330 and 1290 cm^{-1} are shifted to lower frequencies by 10–20 cm^{-1}, while the band at 1360 cm^{-1} is shifted to higher frequencies by 5–10 cm^{-1}. The shifts of these bands could be explained by the implication of noncarboxylic oxygens into the interaction with metal cation.

The bands at 1160–940 cm^{-1} in the spectra of free acid are assigned mainly to the C–O and C–C stretching vibrations. The shifts of these bands to lower frequencies (~5–15 cm^{-1}) observed for the complexes support the assumption that noncarboxylate oxygens of GalA participate in the metal complexation.[52] The intense band at 995–985 cm^{-1}, which appeared only in the vibration spectra of the complex **4** was assigned to the stretching vibration of V=O bonds. The V–O stretching vibration of this complex was found at 487 cm^{-1} (FT-IR) and at 505 cm^{-1} (Raman). The wave numbers of these bands are similar to those reported for oxovanadium(IV) acetylacetonate[53] that confirm the tetragonal pyramidal configuration of the oxovanadium(IV) cations.

The skeletal bands of GalA at ~864 cm^{-1} (weak in IR, strong in Raman) and at 698 cm^{-1} are sensitive to anomeric structure. The former band is shifted to 873–876 cm^{-1} upon complexation. We suggest that this shifted band arose from α-GalA bound to metal cation. Similar band has been observed at 878 cm^{-1} for α-D-galactose but not for β-D-galactose.[54] In contrast, new bands at ~890 and ~475 cm^{-1} arising in the metal complexes indicates β-anomers of metallated GalA. Therefore, vibrational spectra confirm the presence of both anomers in the complexes. Other skeletal bands at ~773, 700, 620 and ~446 cm^{-1} of GalA are also shifted upon complexation that may reflect some conformational changes in the pyranoid ring.

2.5. Vibrational absorption in solutions

The vibrational absorption and VCD spectra of GalA and complexes **1**–**4** in the D_2O and Me_2SO-d_6 solutions are shown in Figure 6. The carboxylic stretching band assignments for the metal/GalA complexes and for free ligand are summarised in Table 5. In the D_2O solution of GalA (pH < 2), the very strong absorption band at 1727 cm^{-1} was assigned to C=O stretching vibration of carboxylic dimers. In Me_2SO-d_6 solution of free ligand, the strong peak at 1740 cm^{-1} with a nonresolved shoulder at 1727 cm^{-1} was observed. The peak at 1740 cm^{-1} was assigned to C=O stretching of carboxylic monomers. Observed shift of C=O stretching band to higher frequencies in the Me_2SO-d_6 solution agrees with the fact that the partial dissociation of hydrogen bonded carboxylic dimers takes place upon dissolving in Me_2SO-d_6. Hydrogen bonding and resonance of carboxylic dimers weaken the C=O bonds, resulting in absorption at lower frequency than observed for the monomer.[45] To compare with the metal complex solutions (pH 5–6), the spectra of the GalA solution in D_2O at pH

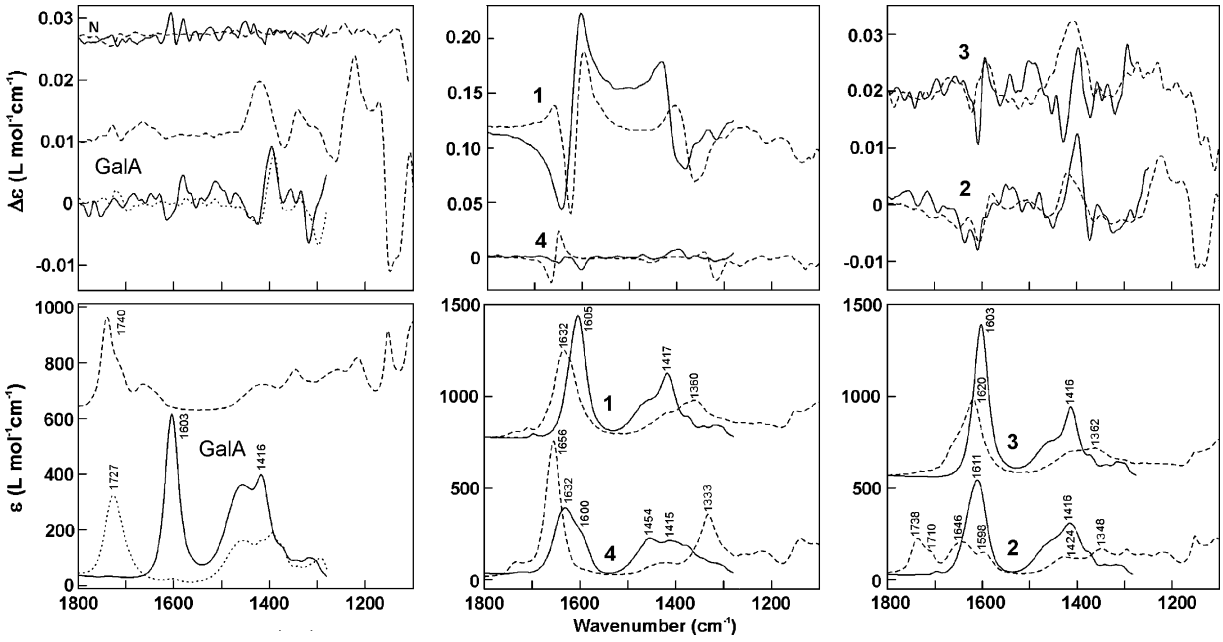

Figure 6. IR absorption (bottom panels) and VCD (top panels) spectra of GalA·H_2O and the metal/GalA complexes **1**–**4** in D_2O pH < 2 (—), pH 6 (····) and in Me_2SO-d_6 (----), the noise spectrum (N).

Table 5. The C=O and COO^- stretching bands of GalA and its metal complexes in D_2O and Me_2SO-d_6 solutions

Solvent	Compound	Wave number (cm^{-1})[a]				
		COOH		COO^-		
		ν(C=O)	ν(C–O)	ν_{as}	ν_s	$\Delta\nu_{as-s}$
D_2O	GalA·H_2O, pH < 2	1727s				
	GalA·H_2O, pH 6			1603s	1416m	187
	1			1605s	1417m	188
	2			1611s	1416m	195
	3			1603s	1416m	187
	4			1632s	1415m	217
				1600sh	1454m	146
Me_2SO-d_6	GalA·H_2O	1740s				
		1727sh				
	1			1632s	1360m	272
	2	1738m	1223w	1646s	1348m	298
		1710w	1260bw	1598m	1424m	174
	3			1620s	1362w	258
	4			1656s	1333s	323

[a] b, broad; m, medium; sh, shoulder; s, strong; v, very; w, weak.

adjusted by NaOD were measured. For pH 6, the carboxylate vibrations $\nu_{as}(COO^-)$ and $\nu_s(COO^-)$ were observed in IR absorption at 1603 and 1416 cm^{-1}, respectively, instead of the C=O stretching band of COOH. These spectral changes confirm the formation of well-dissociated sodium salt of GalA.

IR absorption spectra of the metal/GalA complexes in D_2O and Me_2SO-d_6 solutions had two absorption bands at 1680–1600 and 1454–1333 cm^{-1}. These bands were assigned to $\nu_{as}(COO^-)$ and $\nu_s(COO^-)$ vibrations, respectively (Fig. 6b–e). As in the case of the vibrational spectra of solid complexes, the carboxylate vibrations observed upon complexation instead of the C=O stretching vibration of free GalA confirm the participation of the carboxylic oxygen atoms in metal bonding.[46–50] In D_2O solutions, the asymmetric vibrations of COO^- groups yield a single band at 1603–1611 cm^{-1} in the absorption spectra of complexes **1**–**3**, while complex **4** shows an asymmetric stretching band centred at 1632 cm^{-1} with a shoulder at 1600 cm^{-1}. The tentative assignments of the $\nu_s(COO^-)$ are more obscure due to overlapping with the deformation vibrations related to the COH and CCH groups. All studied complexes in Me_2SO-d_6 solutions give the asymmetric stretching band composed of more or less resolved components (Fig. 6b–e, Table 4). The asymmetric and symmetric stretching bands of carboxylates showed a marked shift to higher and to lower frequencies, respectively. These spectral changes reflect disruption of hydrogen bonds stabilising the structure of the complexes when Me_2SO-d_6 solvent was used instead of D_2O.

From the relatively high values of $\Delta\nu_{as-s} = 258-323\ cm^{-1}$, which were observed in the case of all studied complexes in Me_2SO-d_6 solutions, the unidentate coordination of carboxylate groups to the metal cation can be deduced.[50–58] On the other hand, in D_2O solutions, where $\Delta\nu_{as-s} = 187-217\ cm^{-1}$, the solvent molecules may bridge metal cation and nonbound carboxylate oxygen of GalA supporting pseudobridging coordination of COO^-. For some complexes, however, the additional components observed in the $\nu_{as}(COO^-)$ and $\nu_s(COO^-)$ bands represent $\Delta\nu_{as-s}$ values, which are smaller than that of sodium salt of GalA ($\Delta\nu_{as-s} = 187\ cm^{-1}$). These are complex **2** in Me_2SO-d_6 (174 cm^{-1}) and complex **4** in D_2O (146 cm^{-1}). We assume that the lowering of $\Delta\nu_{as-s}$ observed could be a result of bridging or even bidentate coordination of carboxylates.[50–58]

Complex **2** dissolved in Me_2SO-d_6 showed vibrational bands at 1738 cm^{-1} with a shoulder at 1710 cm^{-1} (C=O stretching of COOH) and at 1646 cm^{-1} with a shoulder at 1598 cm^{-1} (asymmetric stretching of COO^-). We suppose that at least four carboxylic species of this complex that is two bound COO^- and two nonbound COOH, may occur in Me_2SO-d_6 solution. The vibration absorption spectrum of complex **2** freshly dissolved in Me_2SO-d_6 significantly changed during several hours after dissolving (Fig. 7). The absorption decrease occurred in the regions of both asymmetric and symmetric carboxylate stretching vibrations, whereas the bands related to the C=O and C–O stretch of protonated carboxyls markedly increased.

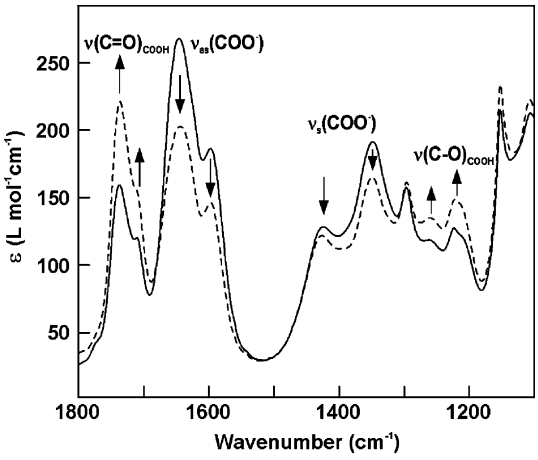

Figure 7. IR absorption spectra of copper(II)/GalA complex **2** freshly dissolved in Me_2SO-d_6 (—) and of the same solution after 5 h (----).

2.6. VCD study

VCD spectroscopy is a technique where the advantages of vibrational spectroscopy are connected with the sensitivity of circular dichroisms to spatial structure of molecules.[59,60] It has been effectively used for conformational studies of chiral small[61–67] as well as large[68,69] biomolecules including carbohydrate derivatives.[70–75] The fact that the most of metal–GalA complexes, in contrast to completely insoluble pectates of polyvalent metal cations, are well soluble in both D_2O and Me_2SO-d_6 is beneficial for the simultaneous vibrational absorption and VCD spectroscopic investigation of these complexes in solutions.

The weak VCD signal in the C=O stretching region was observed in the D_2O (pH < 2) and Me_2SO-d_6 solutions of GalA. In the D_2O solution at pH 6, the weak VCD signal of $\nu_{as}(COO^-)$ was observed in the level of noise (Fig. 6a). In the region 1450–1350 cm^{-1}, where the deformations of the COH and CCH groups overlap the $\nu_s(COO^-)$, the individual VCD bands cannot be resolved and assigned to individual vibrations for both solutions studied. However, the VCD spectra of the D_2O solutions of GalA in this region are independent on pH within the scope of noise level despite the fact that symmetric $\nu_s(COO^-)$ vibrations is manifested in the absorption in this region. The VCD bands observed for the free GalA solutions in the 1450–1300 cm^{-1} region originate therefore mainly in the deformation vibrations of the COH and CCH and are not significantly influenced by the $\nu_s(COO^-)$ vibrations.

The VCD spectra of the metal complexes are presented in two pairs in Figure 6b–e. Note the different $\Delta\varepsilon$ scale used for the spectra of cobalt(II) and oxovanadium(IV) complexes (**1** and **4**) and those of copper(II) and nickel(II) complexes (**2** and **3**), which reflect the different strength of the VCD signals observed. By comparison of the VCD spectra of the free acid and those of the metal complexes (Fig. 6), it is evident that the VCD spectra of the complexes in D_2O differ from that of GalA measured at the same pH in the region of $\nu_{as}(COO^-)$. These differences are even more obvious in Me_2SO-d_6 solutions. Therefore, the observation of optically active species by VCD is related to the complexation. In the region 1350–1450 cm^{-1}, the VCD signal of $\nu_s(COO^-)$ overlaps those of the COH and CCH groups. As a result, the differences in the VCD pattern between free acid and the complexes are evident, they are less pronounced for $\nu_s(COO^-)$ than for $\nu_{as}(COO^-)$ in both D_2O and Me_2SO-d_6 solutions.

The VCD measurements of the cobalt(II) complex **1** in the D_2O and Me_2SO-d_6 solutions give a very strong VCD signal consisting of positive and negative couplets in the $\nu_{as}(COO^-)$ and $\nu_s(COO^-)$ regions, respectively. Although the IR absorption bands in both solutions are not well resolved either by second derivative or self-deconvolution techniques, the well-structured VCD signals were observed. Such enormously enhanced signal, as was seen for complex **1** of this study, has been reported for VCD spectra of cobalt(II) and nickel(II) complexes with *S*-(−)-sparteine and explained by the coupling of low-lying magnetic-dipole allowed d–d transition to the ground state. Explicit explanation of these observations is underway.[76]

Although the copper(II) complex **2** shows the single $\nu_{as}(COO^-)$ absorption band in D_2O, VCD gives two well resolved negative signals at 1610 and 1637 cm^{-1}. In the Me_2SO-d_6 solution, the negative VCD signal at about 1650 cm^{-1} corresponds to main absorption maximum at 1646 cm^{-1}, the positive couplet centred at 1594 cm^{-1} is assigned to absorption maximum at 1598 cm^{-1}.

The nickel(II) complex **3** dissolved in both solvents produces weak VCD signals, moreover the weak solubility in Me_2SO-d_6 causes a low signal-to-noise ratio in the VCD spectra. In D_2O, the positive conservative couplet corresponds to the single absorption $\nu_{as}(COO^-)$ band at 1603 cm^{-1}. In Me_2SO-d_6 the negative VCD signal observed corresponds to the main peak in the absorption $\nu_{as}(COO^-)$ band at 1620 cm^{-1}. The absorption shoulder at 1680 cm^{-1} has no corresponding signal in VCD spectrum. The weak solubility in Me_2SO-d_6 prevents the more detailed view.

A strong positive conservative couplet associated with $\nu_{as}(COO^-)$ was observed for the oxovanadium(IV) complex **4** in Me_2SO-d_6 while two well resolved negative VCD signals are evident in D_2O solutions. The cross-point of the VCD couplet with the zero line observed in Me_2SO-d_6 corresponds to the absorption maximum at 1656 cm^{-1}, whereas the two negative VCD signals in D_2O correspond to the main absorption maximum and the shoulder at 1632 and 1600 cm^{-1}, respectively. In the $\nu_s(COO^-)$ region, the negatively biased VCD doublet corresponding to absorption maximum at 1333 cm^{-1} is observed in Me_2SO-d_6 solution, while the correspondence with absorption bands is more obscure in D_2O solutions.

3. Discussion

In accordance with the results obtained by spectroscopic methods we can provide the structures proposed for the metal/GalA complexes of this study.

3.1. Co^{2+}-galacturonate complex (1)

NMR and vibration spectroscopy indicate the presence of both the α- and β-anomers of GalA in complex **1**. The cobalt(II) cation coordinates ligand anomers in different ways. An addition of complex **1** broadens specifically the ^1H and ^{13}C NMR signals originated from two different sites of α-GalA: the groups C-1,H-1–C-2,H-2 and C-4,H-4–C-5,H-5. These two sites of one α-GalA molecule cannot be simultaneously moved near the cation without breaking the pyranoid ring, so two ligand molecules in different ways of coordination must be involved. In contrast, specific broadening of NMR signals of only C-6 and C-5 carbons and no protons of β-GalA was observed confirming that the β-anomer forms a simple carboxylate complex.

We propose a model of cobalt(II) complexation with two α-GalA molecules, in which noncarboxylate oxygens participate in the cation binding. According to this model, one ligand molecule is coordinated through COO^- and 2-OH groups, and another one through COO^- and 4-OH. In addition, the anomeric hydroxyls 1-OH of both ligands are bound to metal cation through coordinated water molecules (Fig. 8a). The metal–hydrogen and metal–carbon distances of this model are shown in Table 6. It is evident that the atoms, which showed specific broadening of their NMR resonances, are situated close by the cation that is at the distance less than 2.6 nm for hydrogens and less than 2.8 nm for carbons.

Moreover, two differently bound ligand molecules generate a nonsymmetric environment around the cobalt(II) cation that is important for the explanation of the VCD results. Intense and well-structured VCD signals at the asymmetric and symmetric COO^- stretching regions indicate the participation of ligand carboxylates in chiral structures that could arise in the case of α-GalA complex according to the proposal model.

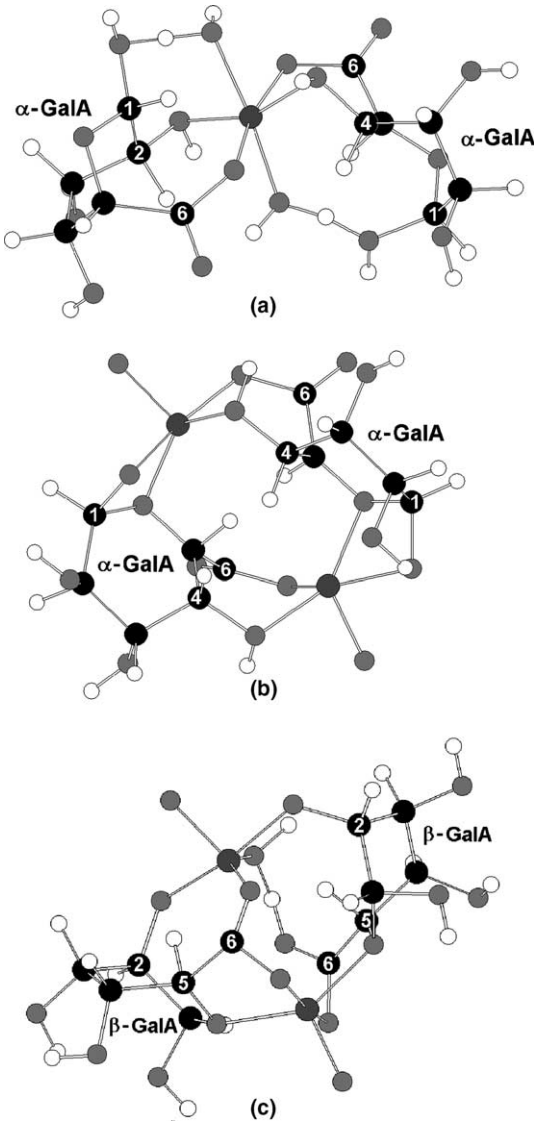

Figure 8. Structures of the metal/GalA complexes **1** (a) and **4** (b, c) proposed according to the molecular mechanics.

3.2. Cu^{2+}-galacturonate complex (2)

Elemental analysis confirms that the metal/ligand molar ratio of complex **2** is 1:2. The complex of such stoichiometry has been observed in the copper(II)/GalA binary system, pH 2.7–6.1.[28] Spectroscopic data confirm that both α- and β-anomers of GalA are present in this complex. We assume that ligand molecules of both anomers coordinate the copper(II) cation by only carboxylate groups. This assumption is in agreement with the NMR results that is specific broadening of only C-6 and C-5 carbons and no protons for both anomers.

Vibrational absorption and VCD spectra confirm that in D_2O solutions the copper(II) complex **2** possesses several types of COO^- coordination assigned to pseudobridging and bidentate modes. After dissolving of **2** in Me_2SO-d_6, however, the carboxylate species partially dissociate with the formation of free protonated carboxylic groups. Instead of carboxylates, the oxo or hydroxo species of GalA bound to copper(II) cations could be formed. The ligand hydroxyls as well as coordinated water molecules may participate as proton donors in such reactions. The absorbance decrease at 740 nm as well as the appearance of the shoulder at 410 nm in UV–vis absorption spectra reflects the changes in electronic configuration of copper(II) cations owing to ligand rearrangement, binding of solvent molecules and (or) removing of bound water from the complex.

3.3. Ni^{2+}-galacturonate complex (3)

The nonspecific broadening of all proton resonances as well as specific broadening of only C-6 and C-5 carbon NMR signals confirms that in complex **3** the ligand molecules of both anomers coordinate nickel(II) cation only through the COO^- groups. In aqueous solutions of this complex, the initially intense absorbance at 354 nm strongly indicates the energy transfer between central ion and ligand molecules, while the subsequent disappearance of this band after dissolving could be a result of the weakness in metal/ligand interactions. Our vibrational absorption and VCD observations of complex **3** in D_2O confirm the formation of the single structure metal complex of pseudobridging COO^- coordination.

3.4. VO^{2+}-galacturonate complex (4)

According to elemental analysis, the molar metal/ligand ratio of complex **4** is 1:1. Specific line broadening of ^1H and ^{13}C NMR spectra indicates that the α- and β-anomers of GalA, which are both present in this complex, bind to oxovanadium(IV) in different ways. The C-1 and C-4 carbons broadened significantly only for α-anomers, suggesting that 1-OH and 4-OH groups participate in the coordination of α-GalA by oxovanadium(IV) cations. The IR absorption and VCD spectra of complex **4** obviously support the formation of at least two carboxylate species in D_2O, which are suggested to be of bridging and unidentate types. In contrast, high values of $\Delta\nu_{as-s}(COO^-)$ and the VCD couplets observed for this complex in Me_2SO-d_6 solution indicate that the coupling of two similar unidentate carboxylates may occur.

On the basis of the results mentioned above we propose two models for complex **4**, one for α-GalA and another for β-GalA (Fig. 8b and c). Both these models are based on the assumption about the dimeric binuclear structure $M_2L_2H_{-4}$ of this complex. The fact that dimeric binuclear species have been observed in the oxovanadium(IV)/GalA binary system[15]support this assumption.

According to the first model, each oxovanadium(IV) cation coordinates one α-GalA through COO^- and 4-OH groups and another α-GalA through O-5 and

Table 6. The hydrogen–metal (H–M) and carbon–metal (C–M) distances (in angstrom) according to the molecular mechanics models (Fig. 8)

Structure	Position	H–M		C–M	
		Left	Right	Left	Right
One Co^{2+} with two α-GalA (**1**)	1	**2.433**	5.228	**2.647**	4.217
	2	**2.390**	5.659	**2.393**	4.630
	3	4.520	4.388	3.895	3.953
	4	5.486	**2.468**	4.439	**2.464**
	5	4.895	**2.587**	3.905	**2.761**
	6			3.058	**2.764**
Two VO^{2+} with two α-GalA (**4**)[a]	1	6.122 (2.961)	3.487 (5.923)	5.100 (**2.586**)	**2.614** (5.166)
	2	6.083 (4.741)	4.403 (6.117)	5.200 (3.964)	3.425 (5.135)
	3	4.669 (5.453)	4.829 (4.520)	4.191 (4.506)	4.025 (4.098)
	4	3.147 (3.612)	2.872 (3.034)	**2.799** (3.697)	3.262 (**2.710**)
	5	**2.457** (**2.290**)	**2.598** (**2.619**)	2.928 (**2.697**)	**2.718** (2.906)
	6			**2.774** (3.655)	4.102 (2.828)
Two VO^{2+} with two β-GalA (**4**)[a]	1	2.961 (3.768)	3.002 (3.780)	2.908 (3.467)	2.913 (3.493)
	2	4.900 (3.826)	4.891 (3.804)	4.033 (3.004)	4.017 (2.999)
	3	5.516 (3.764)	5.462 (3.783)	4.769 (3.775)	4.732 (3.802)
	4	4.903 (4.328)	4.812 (4.392)	4.181 (3.984)	4.119 (4.058)
	5	3.162 (**2.210**)	2.851 (**2.161**)	**2.719** (3.106)	**2.654** (3.192)
	6			**2.469** (**2.737**)	**2.531** (3.326)

[a] Lower (upper) oxovanadium(IV) cation.

deprotonated O-1 (Fig. 8b). Bonded to an anchoring donor group of a sugar ligand like the carboxylate in GalA, the oxovanadium(IV) cation is able to deprotonate easily the hydroxyls and strongly coordinate up to four of them dependently of the pH.[9,13,15–17] The dissociation of the 4-OH group takes place above pH 4,[15] so these groups could be deprotonated in the complex **4**, which was obtained at higher pH. The anomeric hydroxyl of GalA, however, has a more acidic pK_a than the other neutral sugar hydroxyls,[77] so we suggest that the 1-OH group could be deprotonated rather than the 4-OH.

In contrast, the second model assumes that both β-GalA ligands have deprotonated O-2 groups (Fig. 8c). In this model one carboxylate directly bridges two oxovanadium(IV)cations, whereas the other one bridges the second cation indirectly via coordinated water molecule. Such coordination allows the H-5 protons of both ligands to be in proximity to one of the cations.

It is valid for both α- and β-anomeric models of complex **4** that the hydrogen and carbon atoms located close by at least one of the cations demonstrate specific broadening of their NMR resonances. In addition, in both cases the oxovanadium(IV) cations are in distorted tetragonal pyramidal configuration that is in agreement with results of electronic and vibrational spectroscopy.

4. Experimental

4.1. Materials

D-Galacturonic acid monohydrate (Fluka AG, Germany) was used in analysis and in preparation of metal complexes. The pure metal salts $CoCl_2{\cdot}6H_2O$ (Lachema Ltd, Czech Republic), $Cu(NO_3)_2{\cdot}3H_2O$ (Lachema), $NiCl_2{\cdot}6H_2O$ (Lachema) and $VOSO_4$ hydrate (Fluka) were use in preparation of corresponding metal hydroxides. Pure NaOH and Me_2SO were purchased from Lachema. Deuterated solvents that is D_2O (99.96% D) and Me_2SO-d_6 (99.8% D), were purchased from Isosar and Chemotrade, respectively.

4.2. Synthesis

GalA (0.5 g) was dissolved in small volume (2–3 mL) of distilled water. Metal hydroxides were prepared by precipitation with aqueous solution of sodium hydroxide (0.1 mol/L) from the solutions of corresponding salts and washed several times with distilled water. Liquid phase was removed by filtration through paper filter and the solids (metal hydroxides) were washed several times with distilled water before using. Freshly prepared metal hydroxides were added to the solutions of GalA and dissolved by shaking. This procedure was repeated several times until some amount of the metal hydroxides remained nondissolvable. The excess of the metal hydroxides was removed by filtration through paper filter. The complexes were precipitated by 2-propanol or acetone (1:10 v/v) from corresponding filtrates. The sediments were isolated by centrifugation, dried at 40 °C and collected in small flasks. Solid complexes were stored at 4 °C.

4.3. General methods

The carbon and hydrogen contents in GalA·H_2O and solid GalA–metal complexes were measured by

Analyser 2400, CHNS/O, series II (Perkin Elmer, Germany). The content of bound water in the complexes was determined by volumetric Karl Fischer titrator AF8 (ThermoOrion). The content of metal cations was obtained by complexometry: direct titration with 0.02 M EDTA (**1**–**3**) and reverse titration with 0.05 M $ZnCl_2$ after reaction with EDTA (**4**) using indicators murexid (**2**, **3**) and xylenol orange (**1**, **4**).

4.4. Electronic spectroscopic measurement

Electronic absorption spectra (350–900 nm) of the complexes in solutions (1–10 mg/mL) were recorded by UV-4 UNICAM (Thermo Electron, USA) UV–vis double-beam spectrophotometer with bandwidth of 2 nm in 1 cm quartz cell at resolution of 0.5 nm. Diffusion reflectance vis–NIR spectra (400–1200 nm) of solid complexes were measured by NIRSystem spectrometer. The spectra were processed by Vision 3.2 (Thermo Electron, USA) and Origin 6.0 (Microcal Origin, USA) software.

4.5. NMR spectroscopic measurement

^1H and ^{13}C NMR spectra of GalA were measured by Varian Mercury Plus 300 BB (Varian, USA) Fourier transform NMR spectrometer at 22 °C. The solid samples of GalA were dissolved in D_2O (10% w/v). Adjustment to the pH 5.5 were made by adding of 0.1 mol/L NaOD dissolved in D_2O. The metal complexes were added into the solutions of free ligand at the molar ratio 1:1000 mol/mol (complex **1**) and 1:100 mol/mol (complexes **2**–**4**).

4.6. Vibration spectroscopic measurement

Diffuse reflectance FT-IR spectra of the solid samples were obtained using Nicolet 740 spectrometer with DCT 680 (Nicolet Analytical Instruments, USA), 100–200 scans were accumulated with a spectral resolution of 4.0 cm^{-1}. FT-Raman spectra of solid complexes and GalA were recorded by using Bruker FT-Raman (FRA 106/S, Equinox 55/S) spectrometer equipped with a quartz beam splitter, a liquid nitrogen cooled germanium detector and excitation at 1064 nm from a Nd:YAG laser. The laser power was set at 100 mW, and 256 scans were accumulated with a spectral resolution of 2.0 cm^{-1}. vis–Raman spectra were measured by Dilor-Jobin Yvon-Spex (Dilor-Jobin, France) Raman spectrometer equipped with Olympus BX 40 microscope, objective 1003. Argon laser (ν_{ex} = 632 nm, excitation time 120 s, 10 min accumulation per one spectrum, 10 scans) was used for excitation. The spectra were 10-point filtered and polynomial baseline corrected.

IR absorption and VCD spectra of the solutions were recorded on a FT-IR IFS 66/S spectrometer equipped with the VCD/IRRAS module PMA 37 (Bruker, Germany) at resolution of 8 and 4 cm^{-1}, respectively, as described previously.[78] Samples were placed in a demountable cell (A145, Bruker, Germany) composed of two CaF_2 windows separated by a 25 and 50 μm Teflon spacer for measurement in D_2O and Me_2SO-d_6, respectively. The concentrations used for VCD and IR absorption were chosen to be suitable for VCD measurements and were in the range 0.18–0.72 mol/L of GalA. The vibrational spectra presented were expressed in molar absorptivity ϵ (L/mol cm), the spectra of the D_2O solutions were scanned in the region of 1800–1280 cm^{-1} because of strong D_2O absorption below 1280 cm^{-1}. All VCD spectra are the average of three blocks of 5520 scans. OPUS 3.0.17 software (Bruker, Germany) was used for the VCD spectra calculations. The VCD spectra were corrected for baseline, which was obtained as the VCD spectrum of solvent at the same experimental conditions. The noise spectra were calculated as a half of the difference of two following blocks of scans.

4.7. Molecular modelling

Spatial arrangement of the cobalt(II) and oxovanadium(IV) complexes was solved using HyperChem package[79] with MM+ force field. Starting structures were built with the aid of distance constrains derived from NMR spectra. Geometry optimisations were performed at MM+ level and the proper geometry in the final structures was verified using available spectral data, especially for oxovanadium(IV) complexes as the MM+ force field is lacking parameters for this metal.

Acknowledgements

The work was supported by the research grants of Ministry of Education, Youth and Sports of the Czech Republic (CB MSM 223400008) and Grant Agency of the Czech Republic (203/02/0328), and Grant Agency of Academy of Sciences (A4055104).

References

1. Thakur, B. R.; Singh, R. K.; Handa, A. K. *Critical Rew. Food Sci. Nutr.* **1997**, *37*, 47–73.
2. Dronnet, V. M.; Renard, C. M. G. C.; Axelos, M. A. V.; Thibault, J.-F. *Carbohydr. Polym.* **1996**, *30*, 253–263.
3. Kartel, M. T.; Kupchik, L. A.; Veisov, B. K. *Chemosphere* **1999**, *38*, 2591–2596.
4. Grant, G. T.; Morris, E. R.; Rees, D. A.; Smith, P. J. S.; Thom, D. *FEBS Lett.* **1973**, *32*, 195–198.
5. Thom, D.; Grant, G. T.; Morris, E. R.; Rees, D. A. *Carbohydr. Res.* **1982**, *100*, 29–42.
6. Axelos, M. A. V.; Thibault, J.-F. In *The Chemistry and Technology of Pectin*; Walter, R., Ed.; Academic: New York, 1991; p 109.

7. Kohnova, Z.; Kohn, R. *Chem. Listy* **1981**, *75*, 1051–1060.
8. Kohn, R. *Carbohydr. Res.* **1987**, *160*, 343–353.
9. Gyurcsik, B.; Nagy, L. *Coord. Chem. Rev.* **2000**, *203*, 81–149.
10. Whithfield, D. M.; Stojkovski, S.; Bibudhendra, S. *Coord. Chem. Rev.* **1993**, *122*, 171–225.
11. Escandar, G. M.; Sala, L. F. *Can. J. Chem.* **1992**, *70*, 2053–2057.
12. Debongnie, P.; Mestdagh, M. *Carbohydr. Res.* **1987**, *170*, 137–149.
13. Micera, G.; Dessí, A.; Kozłowski, H.; Radomska, B.; Urbanska, J.; Decock, P.; Dubois, B.; Olivier, I. *Carbohydr. Res.* **1989**, *188*, 25–34.
14. Escandar, G. M.; Sala, L. F.; Sierra, M. G. *Polyhedron* **1994**, *13*, 143–150.
15. Garribba, E.; Lodyga-Chruscinska, E.; Sanna, D.; Micera, G. *Inorg. Chim. Acta* **2001**, *322*, 87–98.
16. Branca, M.; Micera, G.; Sanna, D.; Dessi, A.; Kozlowski, H. *J. Chem. Soc., Dalton Trans.* **1990**, 1997–1999.
17. Branca, M.; Micera, G.; Dessi, A.; Kozlowski, H. *J. Chem. Soc., Dalton Trans.* **1989**, 1283–1287.
18. Fuks, L.; Filipiuk, D.; Lewandowski, W. *J. Mol. Struct.* **2001**, *563–564*, 587–593.
19. Fuks, L.; Bűnzli, J.-C. G. *Helv. Chim. Acta* **1993**, *76*, 2992–3000.
20. Angyal, S. J.; Greeves, D.; Littlemore, L. *Carbohydr. Res.* **1988**, *174*, 121–131.
21. Deiana, S.; Gessa, C.; Solinas, V.; Piu, P.; Seeber, R. *Anal. Chim. Acta* **1989**, *226*, 315–322.
22. Aruga, R. *Bull. Chem. Soc. Jpn.* **1981**, *54*, 1233–1235.
23. Grasdalen, H.; Svare, L.; Smidsrod, O. *Acta Chem. Scand. Ser. B* **1974**, *28*, 966–971.
24. Grasdalen, H.; Antonsen, T.; Larsen, B.; Smidsrod, O. *Acta Chem. Scand. Ser. B* **1975**, *29*, 17–25.
25. Antonsen, T.; Larsen, B.; Smidsrod, O. *Acta Chem. Scand.* **1972**, *26*, 2988–2989.
26. Antonsen, T.; Larsen, B.; Smidsrod, O. *Acta Chem. Scand.* **1973**, *27*, 2671–2673.
27. Deiana, S.; Gessa, C.; Solinas, V.; Piu, P.; Seeber, R. *J. Inorg. Biochem.* **1989**, *35*, 107–113.
28. Deiana, S.; Gessa, C.; Manunza, B.; Piu, P.; Seeber, R. *J. Inorg. Biochem.* **1990**, *39*, 25–32.
29. Deiana, S.; Gessa, C.; Piu, P.; Seeber, R. *J. Inorg. Biochem.* **1990**, *40*, 301–307.
30. Deiana, S.; Gessa, C.; Piu, P.; Seeber, R. *J. Chem. Soc., Dalton Trans.* **1991**, 1237–1241.
31. Micera, G.; Deiana, S.; Dessí, A.; Pusino, A.; Gessa, C. *Inorg. Chim. Acta* **1986**, *120*, 49–51.
32. Deiana, S.; Gessa, C.; Usai, M.; Piu, P.; Seeber, R. *Anal. Chim. Acta* **1991**, *248*, 301–305.
33. Branca, M.; Micera, G.; Dessí, A. *Inorg. Chim. Acta* **1988**, *153*, 61–65.
34. Farago, M. E.; Mahmoud, I. E. D. A. W. *Inorg. Chim. Acta* **1983**, *80*, 273–278.
35. Rao, C. R.; Kaiwar, S. P.; Raghavan, M. S. S. *Polyhedron* **1994**, *13*, 1895–1906.
36. Deiana, S.; Erre, L.; Micera, G.; Piu, P.; Gessa, C. *Inorg. Chim. Acta* **1980**, *46*, 249–253.
37. Selbin, J.; Morpurgo, L. *J. Inorg. Nucl. Chem.* **1965**, *27*, 673–678.
38. Etcheverry, S. B.; Williams, P. A. M.; Baran, E. J. *Carbohydr. Res.* **1997**, *302*, 131–138.
39. Luisa, M.; Ramos, D.; Madalena, M.; Caldeira, M.; Gil, V. M. S. *Carbohydr. Res.* **1996**, *286*, 1–15.
40. Filippov, M. P. *Infrared Spectra of Pectic Compounds*; Shtiintsa: Kishinev, 1978.
41. Filippov, M. P. *Kolloid. Zh.* **1980**, *42*, 1208–1211.
42. Filippov, M. P. *Food Hydrocolloids* **1992**, *6*, 115–142.
43. Paterlini, M. G.; Freedman, T. B.; Nafie, L. A. *J. Am. Chem. Soc.* **1986**, *108*, 1389–1397.
44. Pizzini, S.; Bajo, G.; Abbate, S. *Carbohydr. Res.* **1988**, *184*, 1–11.
45. Silverstain, R. M.; Basssler, G. C.; Morrill, T. C. *Spectrometric Identification of Organic Compounds*, 5th ed.; John Willey and Sons, 1997; p 117.
46. Delucas, L.; Bugg, C. E.; Terzis, A.; Rivest, R. *Carbohydr. Res.* **1975**, *19*, 19–29.
47. Tajmir-Riahi, H. A. *Carbohydr. Res.* **1983**, *122*, 241–248.
48. Tajmir-Riahi, H. A. *Carbohydr. Res.* **1983**, *125*, 13–20.
49. Tajmir-Riahi, H. A. *J. Inorg. Chem.* **1988**, *32*, 79–87.
50. Nakamoto, K. *Infrared and Raman Spectra of Inorganic and Coordination Compounds*, 5th ed.; John Wiley and sons: New York, 1997.
51. Etcheverry, S. B.; Williams, P. A. M.; Baran, E. J. *J. Inorg. Chem.* **1996**, *63*, 285–289.
52. Wellner, N.; Kavčuráková, M.; Malovíková, A.; Wilson, R. H.; Belton, P. S. *Carbohydr. Res.* **1998**, *308*, 123–131.
53. Selbin, J. *Chem. Rev.* **1965**, 153–175.
54. Sekkal, M.; Legrand, P.; Vergoten, G.; Dauchez, M. *Spectrochim. Acta* **1992**, *48A*, 959–973.
55. Tackett, J. E. *Appl. Spectrosc.* **1989**, *43*, 483–489.
56. Deacon, G. B.; Phillips, R. J. *Coord. Chem. Rev.* **1980**, *33*, 227–250.
57. Tian, W.; Yang, L.-M.; Xu, Y.-Z.; Weng, S.-F.; Wu, J.-G. *Carbohydr. Res.* **2000**, *324*, 45–52.
58. Nara, M.; Torii, H.; Tasumi, M. *J. Phys. Chem.* **1996**, *100*, 19812–19817.
59. Keiderling, T. A. In *Practical Fourier Transform Infrared Spectroscopy*; Ferraro, J. R., Krishnan, K., Eds.; Academic: San Diego, 1990; pp 203–284.
60. Nafie, L. A.; Freedman, T. B. In *Circular Dichroism Principles and Applications*; Berova, N., Nakanishi, K., Woody, R. W., Eds.; John Wiley and Sons: New York, 2000; pp 97–132.
61. Stephens, P. J.; Devlin, F. J. *Chirality* **2000**, *12*, 172–179.
62. Bouř, P.; McCann, J.; Wieser, H. *J. Phys. Chem. A* **1998**, *102*, 102–110.
63. Solladié-Cavallo, A.; Sedy, O.; Salisova, M.; Biba, M.; Welsch, C. J.; Nafie, L. A.; Freedman, T. B. *Tetrahedron: Asymmetry* **2001**, *12*, 2703–2707.
64. Devlin, F. J.; Stephens, P. J.; Scafato, P.; Superchi, S.; Rosini, C. *Tetrahedron: Asymmetry* **2001**, *12*, 1551–1558.
65. Setnička, V.; Urbanová, M.; Bouř, P.; Král, V.; Volka, K. *J. Phys. Chem. A* **2001**, *105*, 8931–8938.
66. Bouř, P.; Navrátilová, H.; Setnička, V.; Urbanová, M.; Volka, K. *J. Org. Chem.* **2002**, *67*, 161–168.
67. Butkus, E.; Žilinskas, A.; Stončius, S.; Rozenbergas, R.; Urbanová, M.; Setnička, V.; Bouř, P.; Volka, K. *Tetrahedron: Asymmetry* **2002**, *13*, 633–638.
68. Silva, R. A. G. D.; Kubelka, J.; Bouř, P.; Decatur, S. M.; Keiderling, T. A. *Proc. Natl. Acad. Sci. U.S.A.* **2000**, *97*, 8318–8323.
69. Bouř, P.; Záruba, K.; Urbanová, M.; Setnička, V.; Matějka, P.; Fiedler, Z.; Volka, K. *Chirality* **2000**, *12*, 191–198.
70. Back, D. M.; Polavarapu, P. L. *Carbohydr. Res.* **1984**, *133*, 163–167.
71. Bose, P. K.; Polavarapu, P. L. *Carbohydr. Res.* **2000**, *323*, 63–72.
72. Bose, P. K.; Polavarapu, P. L. *Carbohydr. Res.* **1999**, *322*, 135–141.
73. Bose, P. K.; Polavarapu, P. L. *Carbohydr. Res.* **1999**, *319*, 172–183.

74. Bose, P. K.; Polavarapu, P. L. *J. Am. Chem. Soc.* **1999**, *121*, 6094–6095.
75. Setnička, V.; Urbanová, M.; Král, V.; Volka, K. *Spectrochim. Acta Part A* **2002**, *58*, 2983–2989.
76. He, Y.; Cau, X.; Nafie, L. A.; Freedman, T. B. *J. Am. Chem. Soc.* **2001**, *123*, 11320–11321.
77. Liu, Y.; Jiang, X. L.; Cui, H.; Guan, H. S. *J. Chromatogr. A* **2000**, *884*, 105–111.
78. Urbanová, M.; Setnička, V.; Volka, K. *Chirality* **2000**, *12*, 199–203.
79. HyperChem, Release 7.01 for Windows, HyperCube, Inc., 2002.